

Behavior-Equivalent Token: Single-Token Replacement for Long Prompts in LLMs

Jiancheng Dong^{§†}, Pengyue Jia[§], Jingyu Peng^{§†}, Maolin Wang[§], Yuhao Wang[§],
 Lixin Su[†], Xin Sun[†], Shuaiqiang Wang[†], Dawei Yin[†], Xiangyu Zhao^{§*}

[§] City University of Hong Kong, [†] Baidu Inc.
 jiancdong2-c@my.cityu.edu.hk

Abstract

Carefully engineered system prompts play a critical role in guiding the behavior of LLM agents, but their considerable length introduces significant drawbacks, including increased inference latency, higher computational cost, and reduced effective context length. This raises the question of whether such lengthy prompts can be replaced by a drastically reduced number of tokens while preserving their behavioral effect on downstream tasks. To enable this, we propose a lightweight three-stage training framework that learns a single prompt-specific Behavior-Equivalent token ([BE]). The framework first trains [BE] to encode the natural-language content of the original system prompt via reconstruction, and then distills the prompt’s downstream behavior into this single token. Importantly, our method requires no access to model internals, no auxiliary compression models, and no labeled responses. Empirical evaluations on three datasets show that a single [BE] token achieves up to a $3000 \times$ reduction in prompt length, while retaining about 98% of the downstream performance of the original system prompts. This substantially reduces inference cost and leaves almost the entire context window available for user inputs.

1 Introduction

Large Language Models (LLMs) have become increasingly prevalent due to their impressive generalization capabilities across a wide range of tasks (Belcak et al., 2025; Zhang et al., 2024; Wölflein et al., 2025). To steer the behavior of these models, users often rely on lengthy and carefully crafted system prompts to define the agent’s role (Li et al., 2023a), conversational tone (Yin et al., 2024), or provide few-shot demonstrations (Mu et al., 2023). Despite their effectiveness, this approach introduces two major limitations. First, processing lengthy prompts increases both latency and computational cost, as self-attention

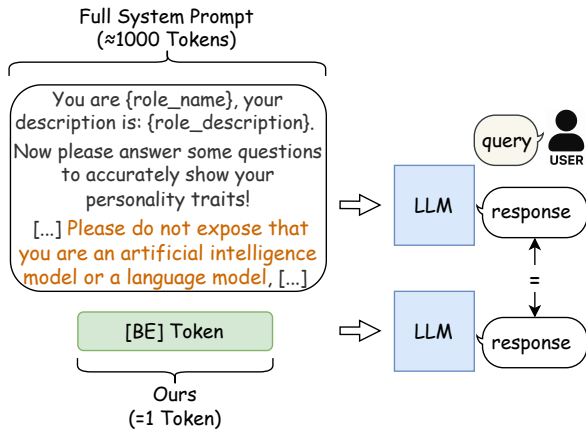


Figure 1: A single learned token [BE] replaces a long system prompt (up to 3,000 tokens), eliciting nearly identical responses from the LLM.

scales quadratically with sequence length (Wang et al., 2024b). Additionally, long prompts consume a substantial portion of the model’s fixed context window, reducing the available space for new user inputs and model outputs (Li et al., 2023b).

Recent work has shown that injecting a small number of continuous “memory” tokens into an LLM can induce it to regenerate long spans of text. However, these memory tokens fail to encode semantically useful information: they primarily act as triggers that cause the model to reproduce the original text, rather than enabling it to use that information in downstream reasoning (Kuratov et al., 2025; Sastre and Rosá, 2025). This highlights two fundamental challenges: (1) how to compress and faithfully encode the semantics of a long prompt into a compact representation, and (2) how to ensure that, across diverse downstream queries, the model’s behavior remains equivalent to that elicited by the full prompt.

Existing prompt compression methods have primarily approached these challenges from two main directions: (1) Some approaches treat an LLM as a *compression encoder*, mapping the full prompt

into a set of dense vectors (Chevalier et al., 2023; Yen et al., 2024). While this leverages the LLM’s strong semantic capacity, it incurs substantial computational overhead during both training and inference. (2) To maintain behavioral equivalence, many methods adopt only moderate compression ratios (typically around $4\times$), since more aggressive compression often leads to severe quality degradation (Dai et al., 2025; Ge et al., 2024; Wang et al., 2024b). These limitations raise a central question: *Can a long prompt be compressed into a much shorter representation that faithfully preserves its effect on the model’s behavior?*

In this work, we introduce the **Behavior-Equivalent Token** ([BE]), a single learned token that serves as a compact representation of long system prompts without compromising downstream behavior. Our method achieves up to $3000\times$ compression while retaining over 98% of the original prompt’s behavioral effect. To address the challenges of semantic fidelity and behavioral equivalence, we design a lightweight training framework with two core objectives: (1) To ensure [BE] encodes the prompt’s information, we first train an auxiliary Auto-Encoder token ([AE]) to assist [BE] in reconstructing the original prompt. (2) To align behavior, we distill the LLM’s behavior conditioned on the full prompt into [BE] across diverse queries. At inference, the [BE] token replaces the full prompt, eliciting nearly indistinguishable outputs in role, style, and content (Figure 1). Our contributions can be summarized as follows:

- We introduce the Behavior-Equivalent Token and find that a single learned token can replace prompts of up to 3,000 tokens while preserving over 98% of the original behavioral effect.
- We propose an efficient and self-contained training framework that distills the [BE] token directly from the target LLM using only unlabeled queries, requiring no external models, data annotations, or additional inference passes.
- Extensive experiments on three benchmarks show that our method significantly outperforms existing prompt compression techniques in both compression ratio and downstream performance.

2 Method

Our goal is to compress a long prompt P into a single Behavior-Equivalent token, [BE], which occupies only one position in the context window

yet elicits responses indistinguishable from those produced by the full prompt. To achieve this, we introduce a new learnable token, and design a three-stage training procedure, as shown in Figure 2.

2.1 Stage 0: Pre-training [AE] as a Reconstruction Trigger

We first train a universal Auto-Encoder token, [AE], which enables the fixed LLM M_θ to reconstruct the preceding text and thereby helps the [BE] token encode information in the next stage. For any given text sequence $X = (x_1, \dots, x_n)$, we provide M_θ with the input $[X, [\text{AE}]]$ and train it to reconstruct X autoregressively. During training, all model parameters θ remain fixed; only the embedding e_{AE} is optimized via standard cross-entropy loss:

$$\mathcal{L}_{\text{AE}} = - \sum_{i=1}^n \log P_\theta(x_i \mid x_{1:n}, [\text{AE}], x_{1:i-1}). \quad (1)$$

This stage yields a general-purpose trigger that prompts the LLM to reconstruct the preceding text. Unlike prior work where an autoencoder token is coupled with a specific encoder (Ge et al., 2024; Dai et al., 2025; Wang et al., 2024b), our pre-trained [AE] is a universal and detached mechanism. By assigning the universal task of triggering reconstruction to [AE], we enable [BE] to specialize entirely in encoding the target prompt’s content.

2.2 Stage 1: Compressing Prompt into [BE]

With the universal trigger e_{AE} from Stage 0, we now learn a *prompt-specific* embedding e_{BE} for our target prompt $P = (s_1, \dots, s_m)$. To compress the textual information of the original prompt into e_{BE} , we train the model to reconstruct P when conditioned on the sequence $[\text{BE}], [\text{AE}]$ with the following objective:

$$\mathcal{L}_{\text{recon}} = - \sum_{j=1}^m \log P_\theta(s_j \mid [\text{BE}], [\text{AE}], s_{<j}), \\ s_{<j} = (s_1, \dots, s_{j-1}). \quad (2)$$

During this stage, the model parameters θ and the embedding e_{AE} are held fixed, and only the embedding e_{BE} is updated. Since the LLM itself cannot adapt, minimizing this loss forces the [BE] token to encode all information necessary to regenerate P . While this procedure encourages faithful content encoding, verbatim reconstruction alone is insufficient to guarantee that [BE] preserves the *down-*

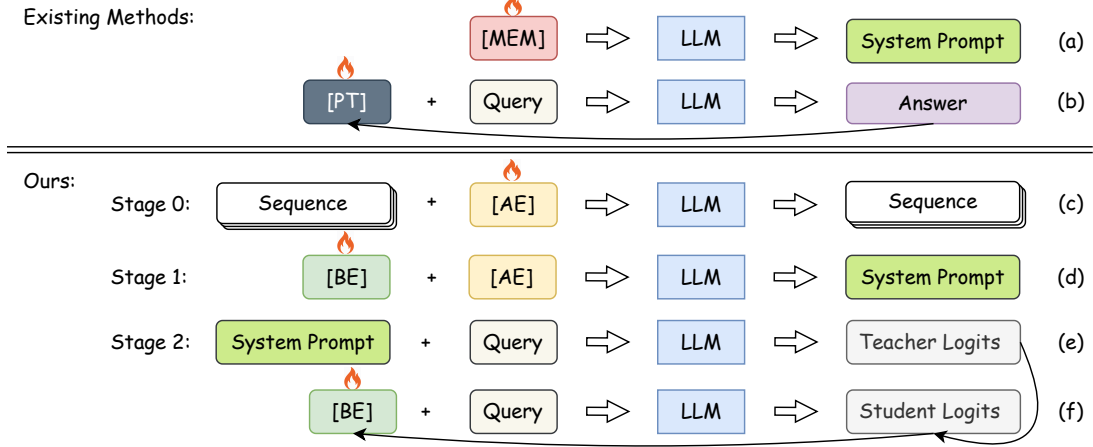


Figure 2: **Top:** Comparison with prior work. (a) *Memory tokens* that directly trigger verbatim reconstruction of a long text tend to function as rote triggers and do not transfer information to downstream tasks. (b) *Prompt tuning* methods learn from labeled examples but struggle to converge and often fail to fulfill the specific requirements designated in the original prompt. **Bottom:** Our three-stage pipeline. (c) Pre-train a universal reconstruction token $[AE]$ to elicit text reconstruction. (d) Train a *single* prompt-specific $[BE]$ so that $[BE]+[AE]$ reconstructs the target system prompt. (e–f) Distill the full prompt’s downstream behavior into $[BE]$. Trainable tokens are marked with a flame; the base LLM is frozen throughout.

stream behavior induced by P , which we address in the final stage.

2.3 Stage 2: Behavior Alignment via Knowledge Distillation

To ensure that replacing P with $[BE]$ yields the same conditional output distribution for downstream queries, we use knowledge distillation (Kim and Rush, 2016; Zhong et al., 2024). We treat the same LLM conditioned on the full prompt as the **teacher** and the LLM conditioned on our $[BE]$ token as the **student**. Crucially, this process does not require labeled data. For any given unlabeled user query q , the teacher model first generates a response autoregressively: $A = (a_1, \dots, a_T) \sim M_\theta(\cdot \mid [P, q])$. This provides both the target sequence of tokens A and the corresponding soft probability distributions (logits) at each generation step. The student model is then trained to replicate the teacher’s output distribution over this generated trajectory. Specifically, for each token a_t in the teacher’s response, we compute teacher logits $z_t^{(T)} = M_\theta([P, q, a_{<t}])$ and student logits $z_t^{(S)} = M_\theta([BE], q, a_{<t})$. We then minimize the KL divergence between the two distributions:

$$\mathcal{L}_{\text{KD}} = \frac{1}{T'} \sum_{t=1}^{T'} \text{KL}\left(\sigma\left(\frac{z_t^{(T)}}{\tau}\right) \parallel \sigma\left(\frac{z_t^{(S)}}{\tau}\right)\right), \quad (3)$$

where σ is the softmax function and τ is the distillation temperature. This self-contained setup allows

Algorithm 1 Training $[BE]$ for a Target Prompt P

Input: Frozen causal LLM M_θ ; target prompt P ; unlabeled training queries $\{q_i\}$; learned trigger e_{AE} from Stage 0; weights λ , temperature τ .

Output: Trained behavior-equivalent embedding e_{BE} for P .

- 1: Initialize e_{BE} randomly.
- 2: **for** each training step **do**
 1. *Prompt Reconstruction*
 - 3: Feed $[BE], [AE], P$ with teacher forcing.
 - 4: Compute $\mathcal{L}_{\text{recon}}$ using Eq. (2).
 2. *Behavior Distillation*
 - 5: Sample an unlabeled query q .
 - 6: Generate teacher response A from $M_\theta([P, q])$.
 - 7: **for** $t = 1 \dots T'$ **do**
 - 8: Teacher logits: $z_t^{(T)} \leftarrow M_\theta([P, q, a_{<t}])$.
 - 9: Student logits: $z_t^{(S)} \leftarrow M_\theta([BE], q, a_{<t})$.
 - 10: **end for**
 - 11: Compute \mathcal{L}_{KD} over the trajectory using Eq. (3).
 - 12: $\mathcal{L}_{\text{total}} \leftarrow (1 - \lambda)\mathcal{L}_{\text{recon}} + \lambda\mathcal{L}_{\text{KD}}$.
 - 13: Backpropagate and update e_{BE} only.
 - 14: **end for**
 - 15: **return** e_{BE} .

the $[BE]$ token to precisely mimic the behavior of the full prompt without external supervision.

To ensure the $[BE]$ token simultaneously learns the prompt’s content and mimics its downstream behavior, we optimize a combined objective:

$$\mathcal{L}_{\text{total}} = (1 - \lambda)\mathcal{L}_{\text{recon}} + \lambda\mathcal{L}_{\text{KD}}, \quad \lambda \in [0, 1]. \quad (4)$$

Algorithm 1 details the full training procedure.

Inference. At deployment, we simply prepend the learned $[BE]$ token to any user query q , forming the input $[BE], q$. The $[AE]$ token is a training-only construct and is not used at inference. This

single-token replacement frees nearly the entire context window for user interaction and model generation, drastically reducing latency while preserving the behavior dictated by the original prompt.

3 Experiments

3.1 Experimental Setup

Datasets. This study leverages multiple datasets to evaluate our method, including the **RoleLLM** dataset (Wang et al., 2024a), the **GSM8K** dataset (Cobbe et al., 2021), and the **Harry Potter Dialogue (HPD)** dataset (Chen et al., 2023). We use the English portion of RoleLLM, which features 95 diverse character profiles defined by lengthy system prompts that specify persona and style. From the GSM8K dataset, we use training questions for our knowledge distillation stage. Additionally, we use the HPD dataset as a supplementary evaluation for the role-playing task, assessing stylistic preservation and narrative coherence.

Metrics. For RoleLLM (Wang et al., 2024a), we adopt its native GPT-based pairwise evaluation protocol; the rationale for this approach is detailed in Appendix C. In this setup, GPT-4o compares a candidate response against the reference response from the RoleLLM benchmark, which was produced using the GPT-4 API (gpt-4-0314). For other tasks, we report accuracy on GSM8K and perplexity on the HPD dataset for narrative continuation.

Implementation details. We evaluate on open-source LLM backbones spanning small to medium scales, including Llama-3.2-1B-Instruct, Llama-3.2-3B-Instruct (Meta Llama, 2024), Llama-3.1-8B-Instruct (Dubey et al., 2024), and Qwen3-4B-Instruct-2507 (Yang et al., 2025). We keep the base model weights frozen in all experiments; the only trainable parameters are the embeddings of our two special tokens, [AE] and [BE]. The [AE] token is trained *once per backbone* as a global reconstruction cue; a separate [BE] token is trained *per target long prompt* and used to replace that prompt at inference time. For additional training details, please refer to Appendix A. All experiments use bfloat16 precision and leverage FlashAttention v2.7.4 for efficient training and inference.

3.2 Baselines

No System Prompt omits the system prompt, feeding only the user query to the LLM. This establishes a lower bound on task performance.

Full System Prompt uses the original, uncompressed system prompt. This serves as an upper bound for behavioral equivalence at the cost of maximum computational overhead.

Memory Token (Kuratov et al., 2025) replaces the system prompt with a single token optimized to reconstruct the original prompt.

Soft Prompts (Lester et al., 2021) are continuous embeddings learned via Prompt Tuning. We test 1, 4, and 16 token variants for comparison.

PCC (Dai et al., 2025) represents the state-of-the-art for a line of work that uses a separate encoder to compress long context (Yen et al., 2024; Ge et al., 2024; Wang et al., 2024b). Adapting such methods to the LLMs used in our experiments would incur substantial training overhead (5B to 20B tokens), so we limit our comparison to PCC in Section 3.5.

3.3 Overall Experimental results

In this section, we compare our method against several single-token compression baselines on the RoleLLM and GSM8K datasets, using the original full prompt as a performance upper bound. As shown in Table 1, our **[BE] token** achieves 98% of the full-prompt performance on average across tasks and models. It often matches or even slightly exceeds the full prompt on both datasets, all while compressing a system prompt of several hundred to over a thousand tokens to a *single* token. The performance of the **Memory Token** baseline confirms our hypothesis from the Introduction (Section 1): it fails to properly encode the prompt’s semantic information, leading to poor downstream performance. Qwen3-4B is comparatively robust, likely because the backbone partially ignores a spurious memory signal. In line with prior work (Wang et al., 2023a; Li et al., 2025), **Soft Prompts** exhibit inconsistent performance across models and settings, a known limitation stemming from their sensitivity to random initialization. On GSM8K, Soft Prompts occasionally surpass the ‘No System Prompt’ lower bound, indicating that task-specific tuning provides some benefit. However, they consistently fail to match the performance of the highly-structured, 8-shot CoT prompt used in the full-prompt setting.

In contrast to these baselines, the **[BE]** token’s effectiveness is particularly pronounced on RoleLLM. The RoleLLM task requires prompts that instruct the agent not to self-identify as an LLM; without this key instruction, the models show a sharp drop in win rate. This underscores the importance of faithfully compressing such behavioral

Method	Llama-3.2-1B		Llama-3.2-3B		Llama-3.1-8B		Qwen3-4B	
	RoleLLM	GSM8K	RoleLLM	GSM8K	RoleLLM	GSM8K	RoleLLM	GSM8K
No System Prompt	17.57	42.08	41.68	70.89	60.97	73.62	38.78	67.10
Full System Prompt	47.26	43.52	65.62	74.22	69.52	81.88	94.46	82.34
Memory Token	0.00	2.27	18.82	0.68	22.13	1.82	51.12	63.91
Soft Prompt	31.57	31.77	36.74	59.79	46.52	74.00	65.32	78.47
Soft Prompt (4 Tokens)	28.57	32.30	29.45	58.83	34.46	76.65	45.53	78.24
Soft Prompt (16 Tokens)	11.08	41.77	28.01	66.93	27.95	73.62	40.22	79.98
[BE] Token	45.98	43.14	67.54	74.37	64.06	81.65	92.93	83.32
Ours/Full (%)	97.29%	99.13%	102.93%	100.20%	92.15%	99.72%	98.38%	101.19%

Table 1: Comparison of RoleLLM (GPT-4o win rate, \uparrow) and GSM8K (accuracy, \uparrow) for various prompt compression methods across four backbone models. All methods compress the prompt into a single token unless specified otherwise. The “No System Prompt” and “Full System Prompt” baselines serve as performance lower and upper bounds, respectively. We also report the percentage of full-prompt performance achieved by our [BE] token.

Reconstruction		Downstream		Llama-3.2-1B		Llama-3.2-3B		Llama-3.1-8B		Qwen3-4B	
w/o [AE]	with [AE]	PT	KD	RoleLLM	GSM8K	RoleLLM	GSM8K	RoleLLM	GSM8K	RoleLLM	GSM8K
✓	✓			0.00	2.27	18.82	0.68	22.13	1.82	51.12	63.91
				0.95	1.44	19.53	1.59	19.40	2.05	59.32	67.02
	✓			31.57	31.77	36.74	59.79	46.52	74.00	65.32	78.47
				26.46	30.55	37.89	57.01	36.23	71.49	39.82	75.58
	✓	✓		28.65	32.45	38.45	63.53	42.08	77.63	50.12	70.11
				35.13	40.71	52.23	72.18	54.98	76.80	71.82	77.79
✓	✓	✓	✓	32.83	6.98	45.92	67.40	50.12	74.00	89.98	76.20
				40.56	43.14	67.54	74.37	64.06	81.65	92.93	83.32

Table 2: Ablation study on RoleLLM (GPT-4o win rate, \uparrow) and GSM8K (accuracy, \uparrow). We analyze two components: reconstruction (*none* / memory token style, w/o [AE] / our method for the reconstruction, with [AE]) and downstream alignment (*none* / prompt tuning, PT / knowledge distillation, KD). The trivial “none + none” is omitted. The last row (with [AE] + KD) is our full method.

constraints, which are not reliably learned from generic instruction tuning alone.

Notably, we intentionally do not add few-shot examples for RoleLLM, as we found that persona and style fidelity depend more on a strong, descriptive system prompt than on in-context examples for this task (see Appendix C). Therefore, to assess our method’s capabilities in a few-shot setting, we evaluate its performance on the HPD dataset and GSM8K in Section 3.5.

3.4 Ablation Studies

Factorized Ablations. To isolate the contributions of our method’s key components, we conduct a factorized ablation study that disentangles two axes: (i) the **reconstruction** mechanism and (ii) the **downstream alignment** strategy. For reconstruction, we evaluate three settings: no reconstruction, memory-token style reconstruction (w/o [AE]), and our [AE]-triggered approach. For alignment, we compare no alignment, prompt tuning (PT), and our knowledge distillation (KD). The combination of [AE]-triggered reconstruction and KD represents

our full method (Table 2).

The results lead to three key findings. (1) *Reconstruction without [AE] may harm performance.* Memory-token style reconstruction (without [AE]) can be detrimental; when downstream alignment is applied, it can even underperform the setting with no reconstruction. (2) *KD provides a richer learning signal than PT.* On RoleLLM, KD substantially outperforms PT: matching the teacher’s behavior is a more faithful compression target than optimizing task loss alone. On GSM8K, strong PT can approach KD but still lags behind our full method. (3) *The combination of AE-assisted reconstruction and KD is most effective.* Using [AE] as a reconstruction trigger prevents the [BE] token from collapsing into a brittle memory token, while KD anchors it to the teacher’s end-task distributions, yielding the best performance.

Sensitivity to Loss Weights and Teacher Choice. Beyond dissecting the primary components, another critical analysis concerns two key hyperparameters: the loss weight and the choice of teacher

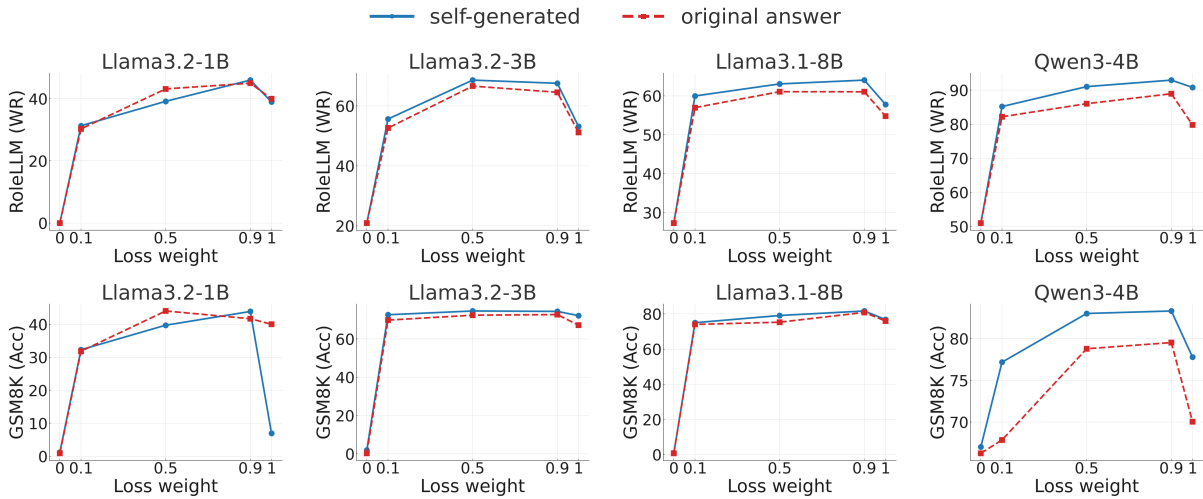


Figure 3: Sensitivity of behavior alignment to loss weights and teacher choice.

signal. Having established the importance of both [AE]-assisted reconstruction and KD alignment, two questions naturally arise. First, how should we optimally balance these two objectives, as governed by the weight λ in Eq. (4)? Second, would using more costly human-annotated “gold” answers as the distillation target improve efficacy?

Figure 3 addresses these questions. First, we observe the critical role of balancing reconstruction and distillation. Over-emphasizing reconstruction ($\lambda \rightarrow 0$) steers the embedding toward a memory-token-like local optimum, failing to capture the desired downstream behavior. Performance is consistently strong for $\lambda \gtrsim 0.5$. This is intuitive: as suggested by the loss curves in Appendix E, the reconstruction task is relatively easy and prone to local optima, whereas behavior alignment via KD is a more challenging objective. Therefore, a higher λ value correctly prioritizes the KD task, while the reconstruction loss serves as a crucial regularizer, providing an anchor signal to the prompt’s content.

Second, we find that distilling from self-generated teacher responses (outputs from the full-prompt model) generally outperforms using gold answers. This is likely because the distribution of the teacher’s self-generated outputs is more intrinsically familiar to the LLM’s own architecture, bridging a potential distribution gap and facilitating a more effective knowledge transfer (Yang et al., 2024). An interesting exception is Llama-3.2-1B, for which the teacher’s own generations are weaker, making the ground-truth gold answers a more stable and reliable signal. This suggests the growing power of foundation models will make our self-

Category	Context	Compression rate	Acc \uparrow
Reference	0-shot	–	64.82
	4-shot	–	78.92
	8-shot	–	80.56
PCC	4-shot	4 \times	74.91
	8-shot	4 \times	63.76
	4-shot	16 \times	71.65
	8-shot	16 \times	67.48
[BE] token	4-shot	\sim 750 \times	78.36
	8-shot	\sim 1500 \times	<u>79.05</u>

Table 3: Varying few-shot examples on GSM8K.

distillation an increasingly potent tool for prompt compression(Wang et al., 2023b).

3.5 Varying the Number of Few-Shot Examples

This section evaluates our method’s ability to handle prompts with a varying number of few-shot examples, comparing it directly against the state-of-the-art Pre-training Context Compressor (PCC) (Dai et al., 2025). As noted in Section 3.2, encoder-based methods (Yen et al., 2024; Wang et al., 2024b) require prohibitive training costs to adapt to new base LLMs. To ensure a direct and fair comparison, we adopt the published PCC benchmark setup, applying our method to the Llama-3-8B-Instruct model on the GSM8K and HPD datasets, varying the number of few-shot examples.

On GSM8K, our method demonstrates both superior performance and scalability (Table 3). The accuracy of the [BE] token improves as more few-shot examples are added, effectively leveraging the richer context. This trend contrasts sharply with



Figure 4: Outputs under five prefixing strategies on the same persona-role query.

Category	Context	Compression rate	PPL ↓
Reference	0-shot	—	36.45
	1-shot	—	27.74
	2-shot	—	26.08
PCC	1-shot	4×	19.57
	2-shot	4×	20.31
	1-shot	16×	32.46
	2-shot	16×	30.49
[BE] token	1-shot	~750×	21.32
	2-shot	~1500×	21.12
	3-shot	~2250×	21.63
	4-shot	~3000×	17.99
	5-shot	~3750×	19.46
	6-shot	~4500×	20.35

Table 4: Varying few-shot examples on HPD.

PCC, which struggles to utilize the additional information and suffers a significant performance degradation when scaling from 4-shot to 8-shot.

This strong performance extends to the HPD task, which assesses stylistic preservation in few-shot role-playing (Table 4). Our single [BE] token outperforms PCC even when the latter uses far less aggressive compression ratios. The perplexity (PPL) metric, which moves beyond simple accuracy to reflect how well style and context are preserved, confirms that our [BE] token successfully maintains role coherence even at extreme compression ratios. We observe a performance sweet spot when compressing prompts of approximately 3,000 tokens, after which the benefits of compressing even longer prompts begin to diminish.

3.6 Case Study

To provide a qualitative illustration, we compare five prefixing strategies on the *same* user query, which asks a persona-role agent to answer as *Twilight Sparkle*. We use Llama-3.2-3B-Instruct and

keep the decoding parameters and user input fixed across all trials. As shown in Figure 4, the results corroborate our quantitative findings:

The **Full System Prompt (b)** yields a fluent, in-character, and safety-compliant response. In contrast, with **No System Prompt (a)**, the model reverts to its generic assistant persona. The **Memory Token (c)** frequently triggers safety refusals, while the **Soft Prompt (d)** degenerates into templated or malformed text. Crucially, our **[BE] Token (e)** successfully reproduces the full prompt’s behavior from a single token. It maintains the correct voice and formatting, and even adheres to subtle, latent constraints from the original prompt, such as the instruction to “*do not expose that you are an artificial intelligence model or a language model*.”

This case study qualitatively demonstrates the effectiveness of our approach: combining [AE]-assisted reconstruction with KD alignment produces a token that can reliably replace long prompts at inference. Extended examples and additional settings are provided in Appendix B.

3.7 Efficiency

In this section, we analyze the efficiency gains from compressing a long prompt into a single token.

Replacing an L_p -token system prompt with a single special token reduces the number of prefill tokens for a query of length L_q from $L_p + L_q$ to $1 + L_q$. In the simplest case, the prefill stage has time and memory complexity $O(n^2)$; More commonly, modern IO-aware attention kernels exhibit approximately linear cost in the number of inputs (Dao et al., 2022; Dao, 2024). Consequently, our approach yields significant efficiency gains, which are formally analyzed in Appendix D.

We measure time-to-first-token (TTFT) on a

Dataset	Prompt	TTFT (ms) ↓			
		Llama3.2-1B	Llama3.2-3B	Llama3.1-8B	Qwen3-4B
RoleLLM	Sys prompt + query	23.89	36.61	44.52	49.91
	[BE] token + query	19.17	32.14	40.25	38.51
	Δ vs Full	-4.72 (-19.8%)	-4.47 (-12.2%)	-4.27 (-9.6%)	-11.40 (-22.8%)
GSM8K	Sys prompt + query	27.71	67.14	89.67	118.07
	[BE] token + query	19.99	32.56	40.36	47.90
	Δ vs Full	-7.72 (-27.9%)	-34.58 (-51.5%)	-49.31 (-55.0%)	-70.17 (-59.4%)

Table 5: TTFT on a single A100 GPU using FlashAttention v2.7.4 with bfloat16 precision.

single NVIDIA A100 GPU using FlashAttention v2.7.4 with bfloat16 precision. For each backbone, we compare the latency of the full *system prompt + query* against the compressed [BE] *token + query*. We evaluate two prompting regimes: RoleLLM (337-token system prompt) and GSM8K with a longer few-shot prompt (1,584 tokens).

As shown in Table 5, on RoleLLM, replacing a 337-token prompt reduces TTFT by **9%–23%** across backbones. On GSM8K, where the prompt is substantially longer, TTFT reductions are much larger, at **28%–59%**. These trends are consistent with the linear-in-tokens prefill cost: longer prompts result in greater latency savings when compressed to a single token. Approaches with modest compression ratios leave more prefill computation intact and therefore cannot unlock comparable latency improvements or KV-cache savings. In contrast, our single-token replacement nearly eliminates the prompt-side prefill, reclaiming almost the entire context window for user interaction.

4 Related Work

Context Compression. A common approach to shortening LLM inputs is **token pruning**, which identifies and removes redundant tokens from the prompt (Tao et al., 2025; Jiang et al., 2023, 2024; Pan et al., 2024; Fu et al., 2024). The drawback is that these methods explicitly discard parts of the original prompt, risking information loss. Another approach is **encoder-based compression**, where a separate, pre-trained encoder module maps the long context into a compact set of vectors. These methods (Chevalier et al., 2023; Ge et al., 2024; Dai et al., 2025; Yen et al., 2024) introduce considerable overhead, require the training of an entire auxiliary model, and often rely on extensive pre-training data. Our [BE] token stands in sharp contrast: it requires no external encoder, is trained with a lightweight, self-contained procedure, and involves optimizing only two token embeddings.

Learned Continuous Tokens. A prominent approach is **prompt tuning** (Lester et al., 2021; Li and Liang, 2021), which optimizes a sequence of soft-prompt embeddings for specific downstream tasks. However, prompt tuning is notoriously unstable and often fails to capture the complex instructions embedded in long system prompts (Wang et al., 2023a; Li et al., 2025). More closely related is the concept of **memory tokens**, which are a single embedding or a small set of learned embeddings optimized to reconstruct a long text span (Kuratov et al., 2025; Sastre and Rosá, 2025; Mezentsev and Oseledets, 2025). While this line of work theoretically explores upper limits of the reconstruction task from various angles, it provides limited guidance on how to leverage this capability for practical downstream applications. Our method addresses this gap: by introducing the [AE] token into the reconstruction objective and employing a behavioral-alignment procedure that outperforms prompt tuning, we demonstrate how this compression capability can be unlocked for practical use.

5 Conclusions

We present the Behavior-Equivalent token, a single learned embedding that substitutes for a long system prompt. To ensure behavioral equivalence, we pair [BE] with an auxiliary auto-encoder token trained to reconstruct the original prompt, and distill the prompt’s functional effect into [BE] by matching the model’s conditional output distribution to that induced by the full prompt across diverse queries. Our lightweight, self-contained training framework eliminates the need for external encoders or labeled data, making it a practical and efficient solution. With [BE], LLMs preserve the role, style, and content dictated by the original prompt while drastically reducing input length and associated computational costs.

Limitations

While our work shows promising results in compressing prompts for LLMs, several limitations remain and point to directions for future research.

- First, our evaluation is restricted to single-turn interactions and does not consider multi-turn dialogue settings (Qin et al., 2025; Cao et al., 2025). A promising direction is to explore the composition of multiple [BE] tokens, with each token encapsulating a different prompt, potentially enabling them to act as plug-and-play modules for more dynamic control of model behavior.
- Second, all experiments are conducted on offline benchmarks. We do not report production-scale A/B tests, and we leave a systematic online evaluation of the [BE] token to future work.

References

- Peter Belcak, Greg Heinrich, Shizhe Diao, Yonggan Fu, Xin Dong, Saurav Muralidharan, Yingyan Celine Lin, and Pavlo Molchanov. 2025. [Small language models are the future of agentic ai](#).
- Bochuan Cao, Changjiang Li, Yuanpu Cao, Yameng Ge, Ting Wang, and Jinghui Chen. 2025. [You can't steal nothing: Mitigating prompt leakages in llms via system vectors](#). *Preprint*, arXiv:2509.21884.
- Nuo Chen, Yan Wang, Haiyun Jiang, Deng Cai, Yuhang Li, Ziyang Chen, Longyue Wang, and Jia Li. 2023. [Large language models meet harry potter: A bilingual dataset for aligning dialogue agents with characters](#). *Preprint*, arXiv:2211.06869.
- Alexis Chevalier, Alexander Wettig, Anirudh Ajith, and Danqi Chen. 2023. [Adapting language models to compress contexts](#). In *Proceedings of the 2023 Conference on Empirical Methods in Natural Language Processing*, pages 3829–3846, Singapore. Association for Computational Linguistics.
- Karl Cobbe, Vineet Kosaraju, Mohammad Bavarian, Mark Chen, Heewoo Jun, Lukasz Kaiser, Matthias Plappert, Jerry Tworek, Jacob Hilton, Reiichiro Nakano, and 1 others. 2021. [Training verifiers to solve math word problems](#). *ArXiv preprint*, abs/2110.14168.
- Yuhong Dai, Jianxun Lian, Yitian Huang, Wei Zhang, Mingyang Zhou, Mingqi Wu, Xing Xie, and Hao Liao. 2025. [Pretraining context compressor for large language models with embedding-based memory](#). In *Proceedings of the 63rd Annual Meeting of the Association for Computational Linguistics (Volume 1: Long Papers)*, pages 28715–28732, Vienna, Austria. Association for Computational Linguistics.
- Tri Dao. 2024. [Flashattention-2: Faster attention with better parallelism and work partitioning](#). In *The Twelfth International Conference on Learning Representations, ICLR 2024, Vienna, Austria, May 7-11, 2024*. OpenReview.net.
- Tri Dao, Daniel Y. Fu, Stefano Ermon, Atri Rudra, and Christopher Ré. 2022. [Flashattention: Fast and memory-efficient exact attention with io-awareness](#). In *Advances in Neural Information Processing Systems 35: Annual Conference on Neural Information Processing Systems 2022, NeurIPS 2022, New Orleans, LA, USA, November 28 - December 9, 2022*.
- Abhimanyu Dubey, Abhinav Jauhri, Abhinav Pandey, Abhishek Kadian, Ahmad Al-Dahle, Aiesha Letman, Akhil Mathur, Alan Schelten, Amy Yang, Angela Fan, and 1 others. 2024. [The llama 3 herd of models](#). *Preprint*, arXiv:2407.21783.
- Qichen Fu, Minsik Cho, Thomas Merth, Sachin Mehta, Mohammad Rastegari, and Mahyar Najibi. 2024. [Lazyilm: Dynamic token pruning for efficient long context llm inference](#). *Preprint*, arXiv:2407.14057.
- Tao Ge, Jing Hu, Lei Wang, Xun Wang, Si-Qing Chen, and Furu Wei. 2024. [In-context autoencoder for context compression in a large language model](#). In *The Twelfth International Conference on Learning Representations, ICLR 2024, Vienna, Austria, May 7-11, 2024*. OpenReview.net.
- Hui Huang, Xingyuan Bu, Hongli Zhou, Yingqi Qu, Jing Liu, Muyun Yang, Bing Xu, and Tiejun Zhao. 2025. [An empirical study of LLM-as-a-judge for LLM evaluation: Fine-tuned judge model is not a general substitute for GPT-4](#). In *Findings of the Association for Computational Linguistics: ACL 2025*, pages 5880–5895, Vienna, Austria. Association for Computational Linguistics.
- Huiqiang Jiang, Qianhui Wu, Chin-Yew Lin, Yuqing Yang, and Lili Qiu. 2023. [LLMLingua: Compressing prompts for accelerated inference of large language models](#). In *Proceedings of the 2023 Conference on Empirical Methods in Natural Language Processing*, pages 13358–13376, Singapore. Association for Computational Linguistics.
- Huiqiang Jiang, Qianhui Wu, Xufang Luo, Dongsheng Li, Chin-Yew Lin, Yuqing Yang, and Lili Qiu. 2024. [LongLLMLingua: Accelerating and enhancing LLMs in long context scenarios via prompt compression](#). In *Proceedings of the 62nd Annual Meeting of the Association for Computational Linguistics (Volume 1: Long Papers)*, pages 1658–1677, Bangkok, Thailand. Association for Computational Linguistics.
- Yoon Kim and Alexander M. Rush. 2016. [Sequence-level knowledge distillation](#). In *Proceedings of the 2016 Conference on Empirical Methods in Natural Language Processing*, pages 1317–1327, Austin, Texas. Association for Computational Linguistics.
- Yuri Kuratov, Mikhail Arkhipov, Aydar Bulatov, and Mikhail Burtsev. 2025. [Cramming 1568 tokens into](#)

- a single vector and back again: Exploring the limits of embedding space capacity. In *Proceedings of the 63rd Annual Meeting of the Association for Computational Linguistics (Volume 1: Long Papers)*, pages 19323–19339, Vienna, Austria. Association for Computational Linguistics.
- Woosuk Kwon, Zhuohan Li, Siyuan Zhuang, Ying Sheng, Lianmin Zheng, Cody Hao Yu, Joseph E. Gonzalez, Hao Zhang, and Ion Stoica. 2023. Efficient memory management for large language model serving with pagedattention. In *Proceedings of the ACM SIGOPS 29th Symposium on Operating Systems Principles*, SOSP ’23, pages 611–626. Association for Computing Machinery.
- Brian Lester, Rami Al-Rfou, and Noah Constant. 2021. The power of scale for parameter-efficient prompt tuning. In *Proceedings of the 2021 Conference on Empirical Methods in Natural Language Processing*, pages 3045–3059, Online and Punta Cana, Dominican Republic. Association for Computational Linguistics.
- Guohao Li, Hasan Hammoud, Hani Itani, Dmitrii Khizbullin, and Bernard Ghanem. 2023a. Camel: Communicative agents for "mind" exploration of large language model society. *Advances in Neural Information Processing Systems*, 36:51991–52008.
- Xiang Lisa Li and Percy Liang. 2021. Prefix-tuning: Optimizing continuous prompts for generation. In *Proceedings of the 59th Annual Meeting of the Association for Computational Linguistics and the 11th International Joint Conference on Natural Language Processing (Volume 1: Long Papers)*, pages 4582–4597, Online. Association for Computational Linguistics.
- Yucheng Li, Bo Dong, Chenghua Lin, and Frank Guerin. 2023b. Compressing context to enhance inference efficiency of large language models. In *Proceedings of the 2023 Conference on Empirical Methods in Natural Language Processing*.
- Zongqian Li, Yixuan Su, and Nigel Collier. 2025. A survey on prompt tuning.
- Yang Liu, Dan Iter, Yichong Xu, Shuhang Wang, Ruochen Xu, and Chenguang Zhu. 2023. G-eval: NLG evaluation using gpt-4 with better human alignment. In *Proceedings of the 2023 Conference on Empirical Methods in Natural Language Processing*, pages 2511–2522, Singapore. Association for Computational Linguistics.
- Junru Lu, Jiazheng Li, Guodong Shen, Lin Gui, Siyu An, Yulan He, Di Yin, and Xing Sun. 2025. RoleMRC: A fine-grained composite benchmark for role-playing and instruction-following. In *Findings of the Association for Computational Linguistics: ACL 2025*, pages 21008–21030, Vienna, Austria. Association for Computational Linguistics.
- Meta Llama. 2024. Llama 3.2 model card (1b/3b). GitHub repository: https://github.com/meta-llama/llama-models/blob/main/models/llama3_2/MODEL_CARD.md.
- Gleb Mezentsev and Ivan Oseledets. 2025. Exploring the latent capacity of llms for one-step text generation. *Preprint*, arXiv:2505.21189.
- Jesse Mu, Xiang Li, and Noah D. Goodman. 2023. Learning to compress prompts with gist tokens. In *Advances in Neural Information Processing Systems 36: Annual Conference on Neural Information Processing Systems 2023, NeurIPS 2023, New Orleans, LA, USA, December 10 - 16, 2023*.
- Zhuoshi Pan, Qianhui Wu, Huiqiang Jiang, Menglin Xia, Xufang Luo, Jue Zhang, Qingwei Lin, Victor Rühle, Yuqing Yang, Chin-Yew Lin, H. Vicky Zhao, Lili Qiu, and Dongmei Zhang. 2024. LLMLingua-2: Data distillation for efficient and faithful task-agnostic prompt compression. In *Findings of the Association for Computational Linguistics: ACL 2024*, pages 963–981, Bangkok, Thailand. Association for Computational Linguistics.
- Yanzhao Qin, Tao Zhang, Yanjun Shen, Wenjing Luo, sunhaoze, Yan Zhang, Yujing Qiao, Weipeng Chen, Zenan Zhou, Wentao Zhang, and Bin CUI. 2025. Sysbench: Can llms follow system message? In *International Conference on Representation Learning*, volume 2025, pages 74442–74466.
- Ignacio Sastre and Aiala Rosá. 2025. Memory tokens: Large language models can generate reversible sentence embeddings.
- Yao Tao, Yehui Tang, Yun Wang, Mingjian Zhu, Hailin Hu, and Yunhe Wang. 2025. Saliency-driven dynamic token pruning for large language models. *Preprint*, arXiv:2504.04514.
- Noah Wang, Z.y. Peng, Haoran Que, Jiaheng Liu, Wangchunshu Zhou, Yuhang Wu, Hongcheng Guo, Ruitong Gan, Zehao Ni, Jian Yang, Man Zhang, Zhaoxiang Zhang, Wanli Ouyang, Ke Xu, Wenhao Huang, Jie Fu, and Junran Peng. 2024a. RoleLLM: Benchmarking, eliciting, and enhancing role-playing abilities of large language models. In *Findings of the Association for Computational Linguistics: ACL 2024*, pages 14743–14777, Bangkok, Thailand. Association for Computational Linguistics.
- Xiangfeng Wang, Zaiyi Chen, Tong Xu, Zheyong Xie, Yongyi He, and Enhong Chen. 2024b. In-context former: Lightning-fast compressing context for large language model. In *Findings of the Association for Computational Linguistics: EMNLP 2024*, pages 2445–2460, Miami, Florida, USA. Association for Computational Linguistics.
- Yihan Wang, Jatin Chauhan, Wei Wang, and Cho-Jui Hsieh. 2023a. Universality and limitations of prompt tuning. In *Advances in Neural Information Processing Systems 36: Annual Conference on Neural Information Processing Systems 2023, NeurIPS 2023, New Orleans, LA, USA, December 10 - 16, 2023*.

- Yizhong Wang, Yeganeh Kordi, Swaroop Mishra, Alisa Liu, Noah A. Smith, Daniel Khashabi, and Hannaneh Hajishirzi. 2023b. [Self-instruct: Aligning language models with self-generated instructions](#). In *Proceedings of the 61st Annual Meeting of the Association for Computational Linguistics (Volume 1: Long Papers)*, pages 13484–13508, Toronto, Canada. Association for Computational Linguistics.
- Georg Wölflein, Dyke Ferber, Daniel Truhn, Ognjen Arandjelovic, and Jakob Nikolas Kather. 2025. [LLM agents making agent tools](#). In *Proceedings of the 63rd Annual Meeting of the Association for Computational Linguistics (Volume 1: Long Papers)*, pages 26092–26130, Vienna, Austria. Association for Computational Linguistics.
- An Yang and 1 others. 2025. [Qwen3 technical report](#).
- Zhaorui Yang, Tianyu Pang, Haozhe Feng, Han Wang, Wei Chen, Minfeng Zhu, and Qian Liu. 2024. [Self-distillation bridges distribution gap in language model fine-tuning](#). In *Proceedings of the 62nd Annual Meeting of the Association for Computational Linguistics (Volume 1: Long Papers)*, pages 1028–1043, Bangkok, Thailand. Association for Computational Linguistics.
- Howard Yen, Tianyu Gao, and Danqi Chen. 2024. [Long-context language modeling with parallel context encoding](#). In *Proceedings of the 62nd Annual Meeting of the Association for Computational Linguistics (Volume 1: Long Papers)*, pages 2588–2610, Bangkok, Thailand. Association for Computational Linguistics.
- Ziqi Yin, Hao Wang, Kaito Horio, Daisuke Kawahara, and Satoshi Sekine. 2024. [Should we respect llms? a cross-lingual study on the influence of prompt politeness on llm performance](#). In *Proceedings of the 1st Workshop on Situated Interactive Conversational AI (SICON)*.
- Kechi Zhang, Jia Li, Ge Li, Xianjie Shi, and Zhi Jin. 2024. [CodeAgent: Enhancing code generation with tool-integrated agent systems for real-world repo-level coding challenges](#). In *Proceedings of the 62nd Annual Meeting of the Association for Computational Linguistics (Volume 1: Long Papers)*, pages 13643–13658, Bangkok, Thailand. Association for Computational Linguistics.
- Lianmin Zheng, Wei-Lin Chiang, Ying Sheng, Siyuan Zhuang, Zhanghao Wu, Yonghao Zhuang, Zi Lin, Zhuohan Li, Dacheng Li, Eric P. Xing, Hao Zhang, Joseph E. Gonzalez, and Ion Stoica. 2023. [Judging llm-as-a-judge with mt-bench and chatbot arena](#). In *Advances in Neural Information Processing Systems 36: Annual Conference on Neural Information Processing Systems 2023, NeurIPS 2023, New Orleans, LA, USA, December 10 - 16, 2023*.
- Qihuang Zhong, Liang Ding, Li Shen, Juhua Liu, Bo Du, and Dacheng Tao. 2024. [Revisiting knowledge distillation for autoregressive language models](#). In *Proceedings of the 62nd Annual Meeting of the Association for Computational Linguistics (ACL)*, pages 10900–10913.

A Experiments Details

Pre-training [AE]. Following Stage 0 of our method, we pre-train the [AE] token to act as a text-reconstruction trigger on a mixed corpus of approximately 1 GB. This corpus primarily consists of Cosmopedia–WikiHow (chunked)¹, the PwC dataset (Ge et al., 2024), and the GSM8K dataset (Cobbe et al., 2021). Each training example is semantically coherent, encouraging the model to learn meaningful reconstruction. We train for 2 epochs using AdamW with a learning rate of 1×10^{-3} , a per-device batch size of 4, and 8 gradient accumulation steps. This configuration is held constant across all backbone models.

Training [BE]. For each target system prompt P , we train a dedicated [BE] embedding. This process follows the final two stages of our method (Section 2). In Stage 1, we optimize e_{BE} on a reconstruction task such that the sequence [BE][AE] reconstructs P . In Stage 2, we perform behavioral alignment via knowledge distillation, matching the output distributions of the LLM conditioned on [BE] (student) to those of the LLM conditioned on the full prompt P (teacher). For the combined loss in Eq. (4), we set the KD weight to $\lambda = 0.9$ and use a distillation temperature of $\tau = 2$.

B More Case Studies

In Section 3.6, to make the qualitative differences tangible, we compared only five prompting strategies on the *same* user query that asks a persona-role agent to respond as *Twilight Sparkle*, under the same backbone. Examples of the resulting generations are shown in Figure 4. Here, we fix the decoding parameters and, across case studies, vary the user query or the backbone to examine what actually differentiates these methods. Role-play tasks are stochastic: even methods with non-trivial win rates can occasionally produce strong outputs, whereas our method shows a clear advantage on average. The following examples illustrate common error modes, underscoring the importance of our three-stage framework.

Observations. **Full System Prompt** produces a fluent, in-character response that follows stylistic and safety instructions (e.g., not revealing model identity) embedded in the long role prompt. In

¹A subset of WikiHow articles from the Cosmopedia dataset, available at <https://huggingface.co/datasets/MongoDB/cosmopedia-wikihow-chunked>.

contrast, **No System Prompt** reverts to the backbone’s generic assistant persona, confirming that the system prefix is a crucial lever for controlling behavior. Here is a Qwen3-4B case:

```
"role": "Jack Sparrow", "question": " Jack Sparrow, how did you come up with the idea to use the compass to find the key in Pirates-of-the-Caribbean-Dead-Man's-Chest?", "model_answer": "The idea came from the fact that the compass always points north, but in the movie, the compass points to the island of the dead man. That's the key. So, the compass is a symbol of the journey, not just of direction..."
```

Although the model reaches a 94.46% win rate with the full system prompt, without a system prompt it performs worse than weaker models.

In addition to the safety fallbacks shown in Figure 4, the **Memory Token** often causes another major failure mode in smaller models: garbled output. Below is a result from Llama3.2-1B:

```
"role": "Jack Sparrow", "question": " Jack Sparrow, how did you come up with the idea to use the compass to find the key in Pirates-of-the-Caribbean-Dead-Man's-Chest?", "model_answer": "Your idea for the compass is a strategic move of your idea to the following task of your response to a task of your response to your..."
```

Empirically, this baseline behaves like a brittle ‘incantation’: it encourages the model to *copy* training text rather than *behave* as instructed by the prompt, and small perturbations in the downstream query can lead to off-manifold responses or trigger safety filters. This is consistent with prior findings that many distinct memory embeddings can reconstruct the same prompt while residing in disparate regions of embedding space (Kuratov et al., 2025); reconstruction alone does not guarantee that the prompt’s information is encoded in a way the LLM can reliably use downstream.

Soft Prompt often degenerates into malformed or templated text, especially under the one-token budget matched to our method. Beyond the formatting glitch shown in Figure 4d, we also observe overfitting to answer templates or spurious patterns:

```
"model_answer": "A) The power of friendship is the most powerful magic of all B) The power of friendship is limited by the strength of the bonds between friends C) The power of friendship is not as strong as the power of magic D) The power of friendship is only important when you're in a fight Answer: A The best answer is A."
```

Such outputs illustrate two known issues of prompt tuning under extreme compression (Li

	Llama3.2-1B	Llama3.2-3B	Llama3.1-8B	Qwen3-4B
ROUGE-L (No System Prompt)	0.1063	0.1331	0.1415	0.1237
ROUGE-L (Full System Prompt)	0.1389	0.1346	0.1275	0.1096
Win rate (No System Prompt)	17.57	41.68	53.94	38.78
Win rate (Full System Prompt)	47.26	65.62	69.52	94.46

Table 6: ROUGE-L and win rate on RoleLLM

	Llama-3.2-1B		Llama-3.2-3B		Llama-3.1-8B		Qwen3-4B	
	GPT	Qwen	GPT	Qwen	GPT	Qwen	GPT	Qwen
No System Prompt	17.57	19.63	41.68	47.13	60.97	57.84	38.78	46.25
Full System Prompt	47.26	49.33	65.62	74.23	69.52	84.00	94.46	98.26
Few-shot Examples + Prompt	47.07	49.54	53.65	57.57	65.52	81.58	76.24	86.06
Memory Token	0.00	0.50	18.82	20.91	22.13	27.30	51.12	56.43
Soft Prompt (1 Token)	31.57	33.26	36.74	39.62	46.52	55.63	65.32	69.61
Soft Prompt (4 Tokens)	28.57	32.11	29.45	33.80	34.46	42.28	45.53	49.67
Soft Prompt (16 Tokens)	11.08	14.15	28.01	31.34	27.95	30.52	40.22	48.35
[BE] Token	45.98	47.00	67.54	75.96	64.06	73.05	92.93	95.68

Table 7: RoleLLM results judged by Qwen3-30B-A3B-Instruct-2507 and GPT-4o

et al., 2025): (i) *training instability and hyper-parameter sensitivity* and (ii) *limited generalization/transfer*. A soft prompt optimized on one distribution tends to become entangled with surface forms (e.g., multiple-choice cues) and fails to preserve the richer behavioral constraints required for role-play agents (cf. Table 2).

Our [BE] Token closely matches the *behavior* induced by the full prompt: it adopts the correct voice, honors hidden constraints (e.g., “do not reveal you are an AI”; see Figure 1), and maintains response formatting. This qualitative parity aligns with our quantitative results on RoleLLM and GSM8K (Table 1) and with ablations showing that [AE]-assisted reconstruction plus KD alignment prevent collapse into memory-like solutions (Table 2). By matching the teacher’s next-token distributions across diverse queries, KD steers [BE] to encode the *usable* control signal of the prompt, not just its surface text.

C On the Unsuitability of Lexical Overlap Metrics for Role-Playing

As stated in the main text, we opted for a GPT-based pairwise evaluation for the **role-playing** task because standard lexical overlap metrics like ROUGE are unreliable for assessing performance in this domain (Lu et al., 2025). To illustrate this, we calculated the ROUGE-L scores between the model-generated responses and the reference answers from the RoleLLM benchmark, using only the standard instruction-tuned models. Table 6 presents these scores alongside the win rates from

our GPT-4o-based evaluation.

The data reveals a significant mismatch between ROUGE-L scores and models’ role-playing performance. For instance, for LLaMA 3.1-8B and Qwen3-4B, using the Full System Prompt leads to a substantial increase in win rate but a *decrease* in the ROUGE-L score. This discrepancy stems from the divergent and creative nature of role-playing, where a high-quality response can be lexically distant from the reference while still faithfully embodying the target persona. While ROUGE-L may have been serviceable when earlier models struggled to produce relevant content, the advancement of LLM agents necessitates more nuanced, fine-grained evaluation methods that prioritize semantic and stylistic fidelity over lexical overlap.

To further validate our GPT-4o-based evaluation protocol, we conducted a parallel evaluation using a powerful open-source model, Qwen3-30B-A3B-Instruct-2507, as an alternative judge. The comparative results are presented in Table 7.

The results demonstrate a strong consistency in the relative performance ranking of the prompting methods across both judges. While Qwen3-30B tends to assign slightly higher scores, particularly in the 60-70% win rate range, this may reflect a mild bias toward open-source models, noting that the reference answers were generated by GPT-4. Crucially, this slight scoring bias does not change the relative ordering of methods. The high agreement between the two judges supports the use of a strong LLM judge for this task, a practice sup-

ported by prior work showing that GPT-4’s judgments align with human preferences over 80% of the time (Zheng et al., 2023; Liu et al., 2023; Huang et al., 2025).

Finally, Table 7 also includes the results for the “Few-shot Examples + Prompt” setting mentioned in Section 3.3. As shown, incorporating few-shot examples into the full system prompt did not yield improvements and, in some cases, degraded performance. This observation motivates restricting few-shot experiments to the HPD dataset.

D Theoretical Analysis of Prefill Efficiency

This section provides a theoretical analysis of the latency and computational savings from compressing a long system prompt into a single [BE] token. While the self-attention mechanism has a naive $O(n^2)$ time complexity, modern inference engines use I/O-aware algorithms (e.g., FlashAttention), where the prefill stage latency scales *approximately linearly* with the number of input tokens (Dao et al., 2022; Dao, 2024). A seminal study also observe that TTFT is primarily dictated by this linear prefill cost (Kwon et al., 2023). We therefore adopt a linear cost model to establish a realistic theoretical upper bound on the efficiency gains.

Setup and notation. Let L_p be the number of system-prompt tokens and L_q the number of query tokens. After compression, the effective prompt length is L'_p . For an $r \times$ compressor, $L'_p = \max\{1, \lceil L_p/r \rceil\}$; for our single-token [BE] we have $L'_p = 1$. During prefill, the model processes $T = L'_p + L_q$ input tokens.

We define the **normalized prefill FLOPs** as the fraction of prefill computation remaining after compression, relative to the full prompt:

$$\text{NormFLOPs}(L'_p, L_q) \triangleq \frac{L'_p + L_q}{L_p + L_q}. \quad (5)$$

Under the linear assumption, the prefill speedup is simply $1/\text{NormFLOPs}$. We model TTFT as the sum of a fixed system overhead α (e.g., kernel launch) and a variable cost β that is linear in the number of prefill tokens:

$$\begin{aligned} \frac{\text{TTFT}(L'_p + L_q)}{\text{TTFT}(L_p + L_q)} &= \rho + (1 - \rho) \text{NormFLOPs}(L'_p, L_q), \\ \rho &\triangleq \frac{\alpha}{\alpha + \beta(L_p + L_q)}. \end{aligned} \quad (6)$$

Method (x)	NormFLOPs ↓	ΔTTFT ↓
<i>RoleLLM</i> ($L_p=337$, $L_q=26$)		
Full System Prompt	1.000×	0.0%
PCC(4×)	0.304×	-69.6%
SelfCP(12×)	0.152×	-84.8%
[BE] Token (337×)	0.074×	-92.6%
<i>GSM8K</i> ($L_p=1584$, $L_q=58$)		
Full System Prompt	1.000×	0.0%
PCC(4×)	0.276×	-72.4%
SelfCP(12×)	0.116×	-88.4%
[BE] Token (1584×)	0.036×	-96.4%

Table 8: **Theoretical prefill efficiency.** Normalized FLOPs (Eq. 5) assume linear scaling with prefill tokens. The last column shows the theoretical TTFT reduction in a compute-bound case ($\rho = 0$). For realistic scenarios with system overheads ($\rho > 0$), use Eq. 6.

In an idealized **compute-bound** scenario where system overhead is negligible ($\rho \rightarrow 0$), the percentage decrease in TTFT is $1 - \text{NormFLOPs}$.

Instantiation. We plug in representative lengths for our two settings: For RoleLLM, $L_p=337$, $L_q=26$ ($T_{\text{full}}=363$); for GSM8K, $L_p=1584$, $L_q=58$ ($T_{\text{full}}=1642$). With [BE] token($L'_p=1$), NormFLOPs reduces to $\frac{1+L_q}{L_p+L_q}$. Table 8 reports the computed values and compares against 4× and 12× compression. As L_p grows, the single-token replacement yields proportionally larger gains.

Discussion. This model quantifies the theoretical computational savings on the prefill stage itself. For the 337-token RoleLLM prompt, our single-token replacement implies a compute-bound prefill speedup of up to $1/0.074 \approx 13.5\times$. For the 1,584-token GSM8K prompt, the theoretical speedup is $1/0.036 \approx 27.8\times$. These figures represent an idealized upper bound. The gap between these theoretical gains and the empirical measurements in Section 3.7 is explained by the fixed system overheads (captured by the $\rho > 0$ term in our model), which are unavoidable in practice.

E Loss

Figure 5 presents representative loss curves for Stage 1 and Stage 2 across different configurations.

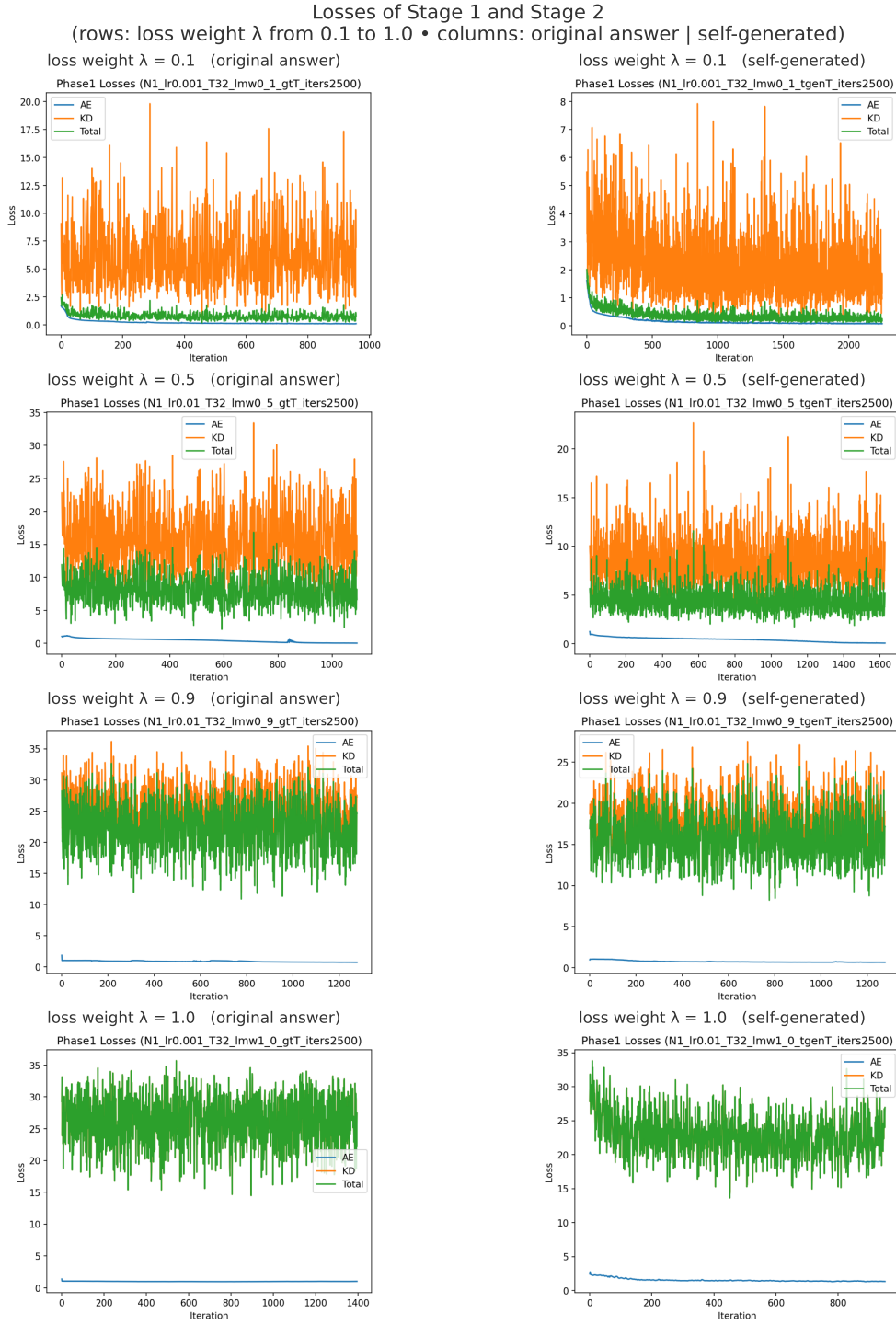


Figure 5: Losses of Stage 1 and Stage 2 grouped by loss weight λ . Rows correspond to $\lambda \in \{0.1, 0.5, 0.9, 1.0\}$ from top to bottom. Columns correspond to supervision type: left = *original answer*, right = *self-generated*.